2013

Gas Bypass and Solids Circulation Rate of an i-CFB Reactor with Coarse Particles

Xingxing Cheng
The University of British Columbia, Canada

Xiaotao T. Bi
The University of British Columbia, Canada

Gas Bypass and Solids Circulation Rate of an i-CFB Reactor with Coarse Particles

Xingxing Cheng and Xiaotao T. Bi*
Fluidization Research Centre, Department of Chemical and Biological Engineering
The University of British Columbia, Vancouver, Canada, V6T 2K9
T: (604) 822-4408. F: (604) 822-6003. E: xbi@chbe.ubc.ca

ABSTRACT: An i-CFB reactor was recently proposed for decoupled NOx adsorption and reduction. In this paper, the hydrodynamic of i-CFB, including gas bypassing and solid circulation rate, was modeled with the results compared with the experimental data. The reactor performances with different distributors, flat, cylindrical and conical, were also studied.

INTRODUCTION

As a promising de-NOx technology, hydrocarbon selective catalytic reduction (HC-SCR) has been widely studied since mid 1980s. To alleviate the negative impact of oxygen on the deNOx performance, a dual adsorption and reduction system has been proposed (1) in which the NOx adsorption takes place in a separate column, decoupled from the catalytic reduction which takes place in another column. A novel HC-deNOx internal circulating fluidized bed (i-CFB) reactor was recently proposed by Yang and Bi (1) in which NOx is adsorbed onto the catalyst surface in the adsorption zone, and then adsorbed NOx is reduced catalytically in the reduction zone, with the catalyst circulating between the adsorption and reduction zones to facilitate the continuous operation.

The performance of the i-CFB reactor is expected to be impacted by the hydrodynamics. Several studies have reported the hydrodynamics of i-CFB reactors, mainly focusing on the measurement of solids circulation rates (2) and the development of correlations for predicting the solid circulation rate (3). These empirical or semi-empirical models could not be applied directly to i-CFBs with different configurations. In this study, gas bypassing and solid circulation rate in a deNOx i-CFB reactor of new configurations were studied in a cold model unit with different distributor configurations, and a hydrodynamics model was developed based on mass and pressure balance.

EXPERIMENTS

A plexiglass i-CFB reactor was constructed with a diameter of 0.1016 m, a draft tube diameter of 0.0508 m and the column height of 1.016 m. The dimensions of the unit were given in (4). Gas was fed to both the draft tube and annulus at different velocities and the bed material circulates between the draft tube and annulus. Three types of distributors, flat, cylindrical and conical plates, as shown in Fig.1, were tested for the gas bypassing and solid circulation. The gap distances for both the flat and cylindrical distributors, H_{G1}, are set to be 10 mm. Two different gap distances, H_G=10 mm and H_G=15 mm, were tested for the conical distributor.

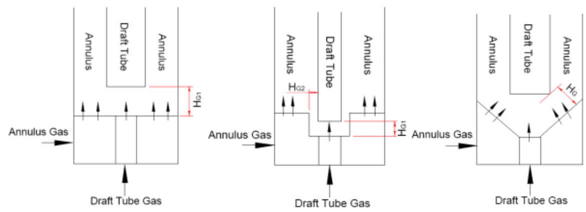

(a) (b) (c)

Fig.1 Distributors for the annulus gas flow. (a): flat; (b): cylindrical; (c): conical

Building air was used as the fluidizing gas. Millet was used as bed material in the test, with the properties shown in Table 1. Two parameters were measured in the experiment, which are gas bypass and solid circulation rate. The gas bypass between the draft tube and the annulus was evaluated by CO_2 tracer method. The solids circulation rate of millet was measured using the visual observation method. The details of the measurement were given in (4).

Table 1 Particle properties

Bed material	**Bulk density (kg/m^3)**	**Average particle diameter (mm)**	**U_{mf} (m/s)**	**U_c (m/s)**	**U_t^{*a} (m/s)**
Millet	837	1.10	0.21	1.28	5.27

Note: *a: calculated by correlation from (5)

HYDRODYNAMIC MODEL OF i-CFB

Mass and pressure balance equations

In an i-CFB, the internal circulation of solids is achieved by the pressure difference between the draft tube and the annulus operating at different superficial gas velocities. Solids mass balance and pressure balance equations are:

$$M_{loading} = M_a + M_d = \rho_s(1-\varepsilon_a)A_a H_a + \rho_s(1-\varepsilon_d)A_d H_d \quad (1)$$

$$U_{sa} \cdot A_a \cdot (1-\varepsilon_a) = U_{sd} \cdot A_d \cdot (1-\varepsilon_d) \quad (2)$$

$$\Delta P_a = \Delta P_d + \Delta P_{or} \quad (3)$$

In a fluidized state, the pressure drop could be expressed by Eqs.4 and 5, which consist of the pressure drops due to gravity, solid acceleration, fluid-wall friction and particle-wall friction.

$$\Delta P_a = H_{effective,a}(1-\varepsilon_a)\rho_p g - 0.5(1-\varepsilon_a)\rho_p u_{p,a}^2 + H_{draft-tube}F_{gw} - H_{draft-tube}F_{pw} \quad (4)$$

$$\Delta P_d = H_{effective,d}(1-\varepsilon_d)\rho_p g + 0.5(1-\varepsilon_d)\rho_p u_{p,d}^2 + H_{draft-tube}F_{gw} + H_{draft-tube}F_{pw} \quad (5)$$

where $H_{effective,a}$ and $H_{effective,d}$ are the effective bed heights in the annulus and draft tube, respectively. Konno and Saito's equation (6) was used to calculate the solid-wall friction and Grbavcic's correlation (7) was used for the gas-wall friction.

Cai's equation (8), which shows good agreement with our experimental bed expansion data, was used to estimate the bed expansion in both the annulus and the draft tube of the i-CFB reactor,

$$\frac{H_f}{H_{mf}} = 1 + \frac{14.33(U - U_{mf})^{0.738} d_p^{\ 1.006} \rho_p^{\ 0.376}}{U_{mf}^{\ 0.937} \rho_f^{\ 0.126}} \quad (6)$$

where H_f is the expanded bed height and H_{mf} is the bed height at minimum fluidization.

Effective bed height

To obtain the effective bed height for Eqs.4 and 5, the flow in the i-CFB was categorized into four different operating modes as shown in Fig.2.

(a): If there is no sufficient bed solid loading or the difference between the gas velocities of annulus and draft tube is too small, solids are not circulated and this flow pattern should be avoided for the operation of i-CFB.

(b): When the solids bed loading or the gas velocity difference in the two zones is increased, the draft tube could be filled up with dilute suspended solids and the solids could start to circulate to the annulus region. In this mode, effective bed height in the draft tube is the same as the draft tube height, and the effective annulus bed height could be calculated from total mass balance.

(c): If the bed loading or gas velocity is further increased, the annulus bed height calculated from mass balance could exceed the height of the draft tube and flow pattern (c) is established. In this case, the effective annulus bed height can still be calculated by mass balance and the effective draft tube bed height is equal to the effective annulus bed height.

(d): When the bed loading or gas velocity is further higher, the bed of the annulus dense bed becomes too high and the dilute jet on top of the draft tube becomes unstable or can no longer penetrate through. The effective draft tube bed height, $H_{effective,d}$, is the sum of draft tube length and jet height, and the effective annulus bed height equals $H_{effective,d}$.

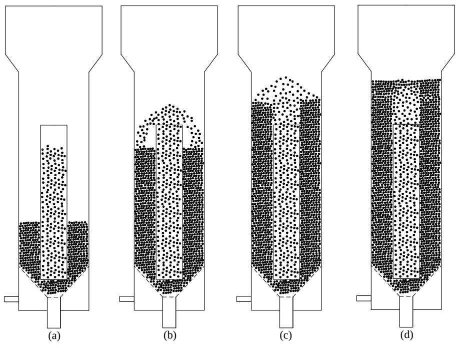

Fig.2 Illustration of four i-CFB flow modes and the effective bed height.

RESULTS AND DISCUSSION

Gas bypass

Due to the pressure difference between the draft tube and annulus and the flow of particles from the annulus into the draft tube at the bottom region, gas can be carried from one region to the other by particles, causing gas bypass and altering the actual gas flow in each region. The amount of gas partitioning into the annulus and draft tube from their inlets could affect the flow rate of both zones and further affect the solid circulation rate. Furthermore, in the i-CFB reactor, the bypass of gas could change the oxygen concentrations in the catalytic reduction zone, affecting the reaction performance.

Table 2 Gas bypass correlations for different distributors

Distributor	R_{AD}	R_{DA}
Flat H_G=10 mm	$R_{AD}=0.880\left(\frac{U_a}{U_{mf}}\right)^{0.446}\left(\frac{U_d}{U_{mf}}\right)^{1.55}$	$R_{DA}=129\left(\frac{U_a}{U_{mf}}\right)^{-1.56}\left(\frac{U_d}{U_{mf}}\right)^{--1.40}$
Cylindrical H_G=10 mm	$R_{AD}=0.930\left(\frac{U_a}{U_{mf}}\right)^{1.78}\left(\frac{U_d}{U_{mf}}\right)^{0.849}$	$R_{DA}=6.4\times10^{6}\left(\frac{U_a}{U_{mf}}\right)^{-5.43}\left(\frac{U_d}{U_{mf}}\right)^{-3.31}$
Conical H_G=10 mm	$R_{AD}=0.676\left(\frac{U_a}{U_{mf}}\right)^{0.193}\left(\frac{U_d}{U_{mf}}\right)^{1.55}$	$R_{DA}=857\left(\frac{U_a}{U_{mf}}\right)^{-0.102}\left(\frac{U_d}{U_{mf}}\right)^{-1.86}$
Conical H_G=15 mm	$R_{DA}=149\left(\frac{U_a}{U_{mf}}\right)^{0.587}\left(\frac{U_d}{U_{mf}}\right)^{-0.782}$	$R_{DA}=583\left(\frac{U_a}{U_{mf}}\right)^{-0.65}\left(\frac{U_d}{U_{mf}}\right)^{-1.34}$

The gas bypass ratio, both from the annular region to the draft tube (R_{AD}) and from draft tube to annular region (R_{DA}), was measured at different gas velocities for the i-CFB with different distributor configurations (4). The data are then correlated as a function of the draft tube gas velocity, U_d, and annulus gas velocity, U_a, with the results shown in Table 2. Those correlations will be coupled into the hydrodynamics model to predict the solid circulation rate.

Solid circulation rate

The solid circulation rate was measured for different reactor configurations with the data shown in Fig.3.

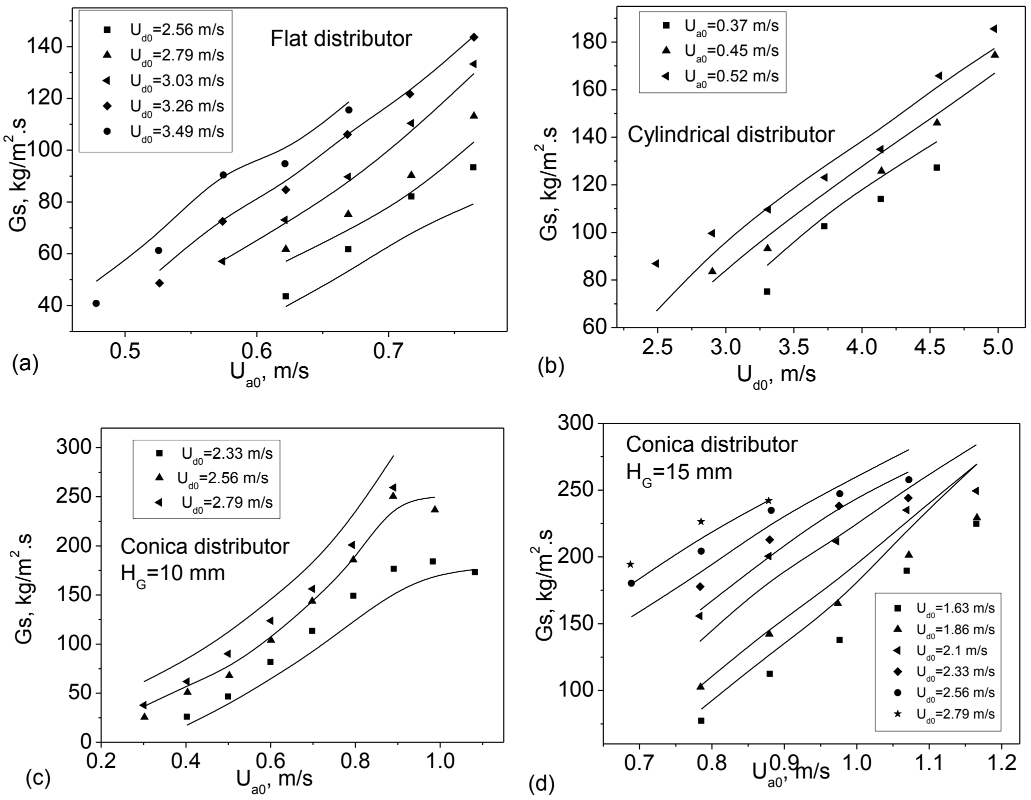

Fig.3 Solid circulation rates at different inlet velocities for different configurations: (a): flat distributor; (b): cylindrical distributor; (c): conical distributor, H_G=10 mm; (d): conical distributor, H_G=15 mm. (symbols: experimental data (4); lines: model fitted)

Based on the gas bypassing correlations, the real gas velocities in the annulus and draft tube could be calculated. The voidage in both zones could then be obtained, followed by the calculation of pressure drop over each zone using Eqs.4 and 5, respectively. The pressure drop across the orifice could be obtained from the overall pressure balance (Eq.3).

It has been reported that the pressure drop for gas-solids two-phase flow across the orifice could be generally expressed as Eq.7, as derived from

Bernoulli's equation for single phase flow (2, 9). This equation showed good agreement with the experimental values in Kim's group for i-CFBs (2, 3), with C_D ranging from 0.3-0.4.

$$G_S = C_D \left(A_{or} / A_a \right) \left[2 \rho_a \Delta P_{or} \right]^{0.5} \tag{7}$$

In this study, the annulus of the i-CFB operates as a moving bed at low values of U_a. Thus voidage in the annulus is quite close to the voidage at minimum fluidization. According to Eq.7, G_s is linearly proportional to $(\Delta P_{or})^{0.5}$, since all the other parameters are more or less remain as constants. Values of G_s and $(\Delta P_{or})^{0.5}$ plotted in Fig.4show that the performances of different distributors differ significantly. The cylindrical distributor shows the best fitting with Eq.7. However, no linear relationship with $(\Delta P_{or})^{0.5}$ was observed for G_s values of i-CFB with a flat distributor. Even for the same type of conical distributor, G_s values from H_G=15 mm shows better fitting with Eq.7 than the values from H_G=10 mm. Overall, it is unlikely that a single C_D value could be fitted to the experimental data for each distributor.

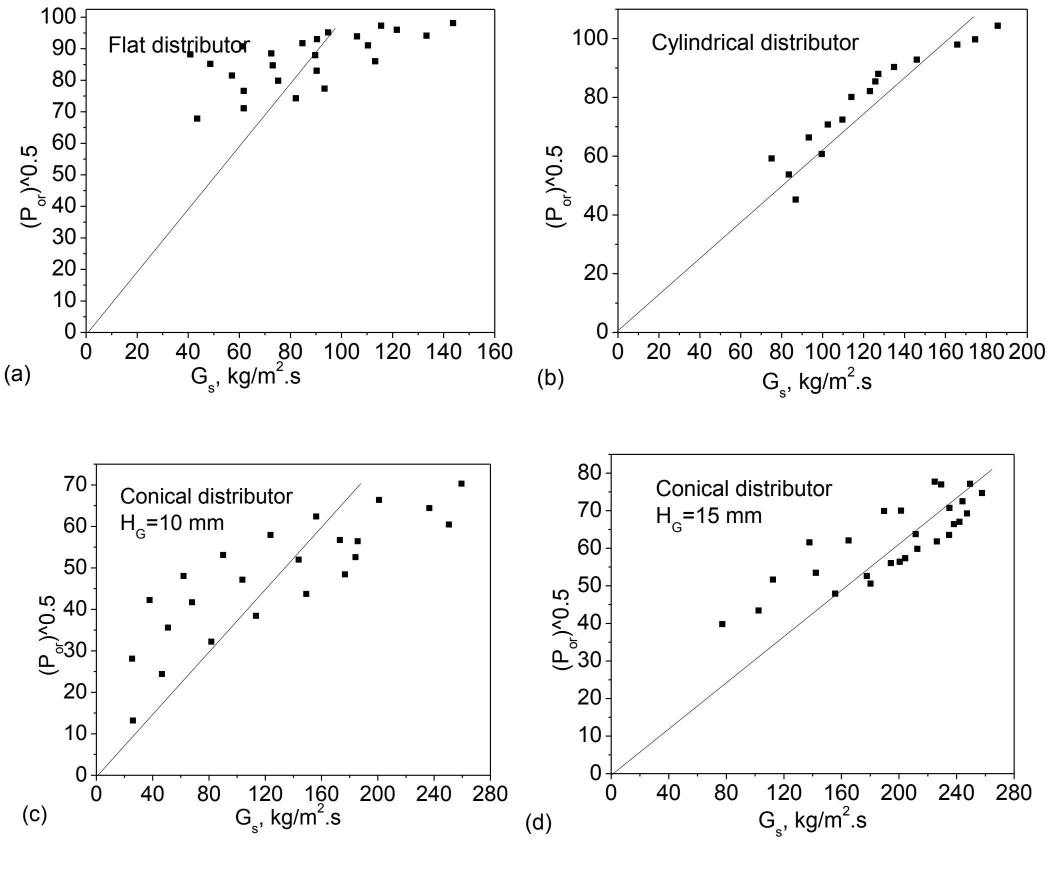

Fig.4 Plot of $(\Delta P_{or})^{0.5}$ as a function of G_s for different configurations: (a): flat distributor; (b): cylindrical distributor; (c): conical distributor, H_G=10 mm; (d): conical distributor, H_G=15 mm;

To further explore the characteristics of C_D, C_D values fitted from each data point were plotted in Fig.5 as a function of Reynolds numbers based on particle velocity through the orifice, with the definition given in Eq.8. It is observed that all the C_D values increase almost linearly with Re_p for all the configurations, with the obtained linear correlations given in Eqs.9 to 12.

$$\mathrm{Re}_p = \frac{\rho_g d_p U_{p,a}}{\mu} \tag{8}$$

Flat distributor: $C_D = 0.0245\mathrm{Re}_p + 0.0168 \quad R^2 = 0.93$ (9)

Cylindrical distributor: $C_D = 0.0113\mathrm{Re}_p + 0.0879 \quad R^2 = 0.92$ (10)

Conical distributor, H_G=10 mm: $C_D = 0.0405\mathrm{Re}_p + 0.0844 \quad R^2 = 0.82$ (11)

Conical distributor, H_G=15 mm: $C_D = 0.0261\mathrm{Re}_p + 0.1276 \quad R^2 = 0.63$ (12)

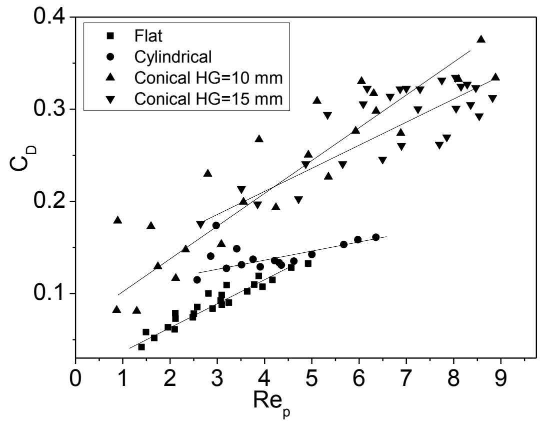

Fig.5 C_D as a function of Re_p for different configurations.

The simulated results using the fitted C_D values in Eqs. 9-12 are also plotted in Fig.3. This model will be used for the modeling and simulation of the reactor performance of the i-CFB reactors for catalytic reduction of NOx using hydrocarbon reductants.

CONCLUSIONS

Hydrodynamics in an i-CFB with different distributor configurations, flat, cylindrical and conical, was studied. A hydrodynamic model was developed based on the pressure/momentum balance and mass balance. Gas bypass was also considered in the model. Particle discharge coefficients of the orifice of different distributors were obtained by fitting with the experimental data. The model showed good agreement with the measured solids circulation data for all the configurations studied.

NOMENCLATURE

A	Cross sectional area, m^2	ε	Voidage
C_D	Drag force coefficient	ρ	Density, kg/m^3
d	Diameter, m	μ	Viscosity, Pa.s
F	Frictional force, Pa/m	Subscript	
G_s	Solid circulation rate, $kg/m^2.s$	a	Annulus
H	Bed height, m	d	Draft tube
M	Mass of solids, kg	AD	Annulus to draft tube
ΔP	Pressure drop, Pa	DA	Draft tube to annulus
R	Gas bypass ratio, %	p	Particle
Re	Reynolds number	g	Gas
U	Velocity, m/s	or	Orifice

REFERENCES

(1). T. T. Yang and H. T. Bi, A novel fluidized bed reactor for integrated NOx adsorption-reduction with hydrocarbons, Environ. Sci. Technol., 2009. 43(13): 5049-5053.

(2). J. H. Jeon, S. D. Kim, S. J. Kim, and Y. Kang, Solid circulation and gas bypassing characteristics in a square internally circulating fluidized bed with draft tube, Chem Eng Process, 2008. 47(12): 2351-2360.

(3). S. D. Kim, Y. H. Kim, S. A. Roh, and D. H. Lee, Solid circulation characteristics in an internally circulating fluidized bed with orifice-type draft tube, Korean J. Chem. Eng., 2002. 19: 911–916.

(4). T. T. Yang, A novel fluidized bed reactor for integrated NOx adsorption-reduction with hydrocabons, in Department of chemical and biological engineering. 2008, University of British Columbia: Vancouver.

(5). D. Kunii and O. Levenspiel, Fluidization Engineering. 1991, Massachusetts: Butterworth-Heinemann.

(6). H. Konno and S. Saito, Pneumatic conveying of solids through straight pipes, J. Chem. Eng. Jpn, 1969. 2: 211-217.

(7). Z. B. Grbavcic, D. V. Vukovic, S. D. Jovanovic, R. V. Garic, D. E. Hadzismajlovic, H. Littman, and M. H. Morgan, Fluid-Flow Pattern and Solids Circulation Rate in a Liquid-Phase Spout Fluid Bed with Draft Tube, Can J Chem Eng, 1992. 70(5): 895-904.

(8). P. Cai, G. D. Michele, and A. T. Gradassl, A generalized method for predicting gas flow distribution between the phases in FBC, Fluidized bed combusiton, 1993. 2: 991-1002.

(9). M. Kuramoto, D. Kunii, and T. Furusawa, Flow of Dense Fluidized Particles through an Opening in a Circulation System, Powder Technology, 1986. 47(2): 141-149.